International Journal of
Intelligent Systems and
Applications in Engineering
ISSN:2147-6799 www.atscience.org/IJISAE
Advanced Technology and Science
Original Research Paper

The Assessment of Time-Domain Features for Detecting Symptoms of Diabetic Retinopathy

Gülin Elibol*[1], Semih Ergin[2]

Accepted 3rd September 2016

Abstract: Diabetes affects the capillary vessels in retina and causes vision loss. This disorder of retina due to diabetes is named as Diabetic Retinopathy (DR). Diagnosing the stages of DR is performed on a publicly available database (DiaraetDB1) via detecting the symptoms of this disease. Time-domain features are extracted and selected to classify a fundus image. Fisher's Linear Discriminant Analysis (FLDA), Linear Bayes Normal Classifier (LDC), Decision Tree (DT) and k-Nearest Neighbor (k-NN) are used as the classification methods in the experimental benchmarking. The recognition accuracies are obtained using all features (68 features) and selected features separately. k-NN is observed as the best classification method for without feature selection case and it gives averagely 92.22% accuracy. For feature selection case, LDC gives the best average accuracy as 92.45% with maximum 7 carefully chosen features.

Keywords: *Sequential feature selection, diabetic retinopathy, microaneurysms, hemorrhages, exudates.*

1. Introduction

Insufficient generation or low level of insulin causes the diabetes. This disease affects many parts of body, more particularly affects blood vessels of a retina. Diabetic Retinopathy (DR) is resulted from the damage of tiny blood vessels inside diabetic patient's retina [1]. DR is a major cause of vision loss and blindness [2]. It has four stages that are mild non-proliferative, moderate non-proliferative, severe non-proliferative and proliferative. Besides, an early diagnosis can prevent a permanent visual disability.

Diagnosing DR is realized via detecting the symptoms of retinopathy from fundus (retinal) images that show the posterior part of eye. The symptoms of this disease are called as microaneurysms (MA), hemorrhages (HR), soft exudates (SE) and hard exudates (HE). Microaneurysm is the quite first symptom of DR. Due to a loss of pericyte, capillary vessels protrude and red small dots occur on the top layer of retina [3]. Microaneurysm also refers as red small dots. The second symptom is hemorrhages. The vessels are bleed due to lack of feeding. Their appearances are similar to microaneurysm, but they are shown at the inner layer and outer plexiform [4]. Another symptom is soft exudates. It occurs when the layer of nerve fiber is clogged because of small arteries choked. Soft exudates are also known as cotton-wool spots [5]. Soft exudates are mostly confined with micro-aneurysm and vessels that are hyper-permeable. The last symptom is hard exudates. They are accumulation of yellow fat and protein that are seeping from capillary vessels and microaneurysms [6]. These symptoms of DR are shown in Fig. 1 [7].

The early stage of this disease is mild non-proliferative DR. In this stage, microaneurysms occur at the retinal vessels. The next stage is moderate non-proliferative and micro-aneurysms are increased, hemorrhages and hard exudates are started during this stage. The third stage is severe non-proliferative DR. The lack of oxygen became apparent in retina and then hemorrhages and hard exudates are increased. In this stage, the scar tissue that is leading the visual loss is occurred. The last stage is proliferative DR and the new unhealthy vessels are started to generate due to the increase in lack of oxygen and lack of feeding. These new vessels are very delicate and started to bleed and then they may cause to a visual loss at any moment.

In literature, diagnosing the stages of DR is starting with detecting MA. In [8], a three-stage system is proposed to detect MA via using filters. First of all, the candidate regions of MA are determined from fundus images and then 15 features are extracted from these regions to classify MA. Those features are area, eccentricity, perimeter, compactness, mean, standard deviation, homogeneity, etc. A feature selection is not performed and hybrid classifier that combines Gaussian Mixture Model (GMM) and Support Vector Machine (SVM) is used. Another method for classifying DR is the detection of HR. In this methodology, HR is detected and then it is classified into three classes which are normal, moderate, severe non-proliferative DR [9]. Random Forests Tree is used for classification and eventually the proposed system has 90% accuracy while moderate and severe non-proliferative cases were 87.5% accurate. In [10], MA and HR are both detected for non-proliferative stages of DR. A geometric-based criteria, which are size, shape, roughness, edge sharpness, colour, depth, etc., are used to classify HR and MA. In this study, the stage of DR is determined according to the number and location of them. Ultimately, the suggested system achieves sensitivity and specificity values of 89.47% and 95.65% for the classification of DR versus normal. Neural Network (NN) is used to classify moderate, severe non-proliferative, proliferative DR and normal stages using features such that red, green, blue layer perimeter, and area [11]. The proposed system gives more than 80% accuracy. In addition to these, detecting exudates also gives information about non-proliferative DR. In [12], hard exudates are detected and then mean, standard deviation, compactness, size, edge strength, etc.

[1] *Department of EEE, Eskisehir Osmangazi University, Eskisehir, Turkey*
[2] *Department of EEE, Eskisehir Osmangazi University, Eskisehir, Turkey*
* *Corresponding Author: Email: gelibol@ogu.edu.tr*
Note: This paper has been presented at the 3rd International Conference on Advanced Technology & Sciences (ICAT'16) held in Konya (Turkey), September 01-03, 2016.

features are extracted from RGB fundus images. Multi-layer perceptron is applied and the given approach yields a 100% mean sensitivity, 84.0% mean specificity and 92.0% mean accuracy. Hard and soft exudates are identified and features are extracted using Gray Level Co-occurrence Matrix [13]. Entropy, contrast, energy and homogeneity are used as features and SVM is applied to classify fundus images into moderate and severe non-proliferative DR.

In this paper, the aim is to detect the symptoms of diabetic retinopathy. These symptoms are MA, HR, HE and SE. DIARETDB1 database, which is publicly available, includes 89 different retina images (fundus) including all symptoms. A new database is generated with five different classes for each symptom and normal (healthy) retinas. 17 time-domain features are extracted through four different window sizes constituted from each retina image. The features which have more discrimination power are selected via Sequential Forward Feature Selection (SFS) method. Fisher's Linear Discriminant Analysis (FLDA) [14], Linear Bayes Normal Classifier (LDC) [15], Decision Tree (DT), and k-Nearest Neighbor (k-NN) are utilized as the classification algorithms to benchmark [16, 17].

The rest of the paper is organized as follows: Section 2 presents the extraction of features from fundus images. Section 3 explains the used classification algorithms briefly. Section 4 presents the experimental work. Finally, conclusions and future work are given in Section 5.

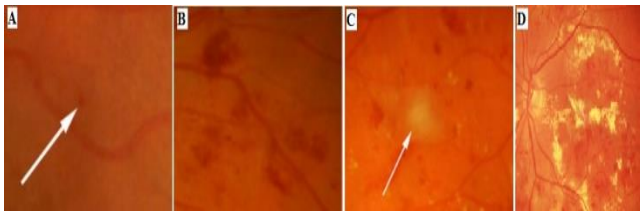

Figure 1. Symptoms of Diabetic Retinopathy: microaneurysm (A); Hemorrhages (B); soft exudates (C); hard exudates (D).

2. Feature Extraction

Time-domain features are extracted using gray values of pixels [18]. 17 features are extracted from each fundus image for one window size. 3x3, 5x5, 7x7 and 9x9 windows are formed, therefore 68 features ($f_1, f_2, \dots, f_{67}, f_{68}$) are obtained for each fundus image. An example of utilized non-proliferative gray level images is shown in Fig. 2. For normal (healthy) retinas, the values of all pixels in the utilized image are zero. The whitish pixels are indicated the parts for symptoms of MA, HR, SE and HE.

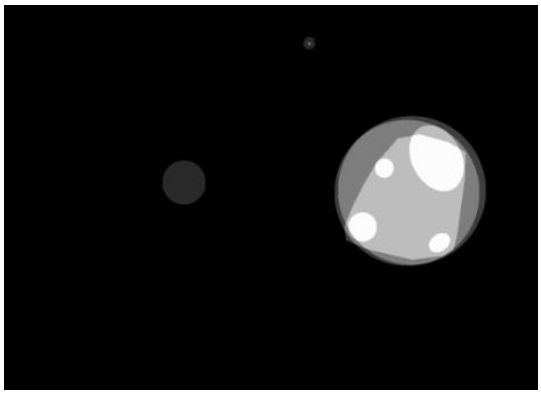

Figure 2. Non-Proliferative Gray Level Fundus Image

Figure 3. Normal (Healty) Gray Level Fundus Image

The extracted features are calculated from the pixel values in the corresponding window. For each window size (2r+1 x 2r+1), the center pixel of the window is located at (pr+1, pr+1) and the other indices of the pixels are shown in Fig. 4 and the extracted features for each window size are given in Table 1 [18].

$p_{r-3,r-1}$	$p_{r-3,r}$	$p_{r-3,r+1}$	$p_{r-3,r+2}$	$p_{r-3,r+3}$
$p_{r-2r,r-1}$	$p_{r-2r,r}$	$p_{r-2r,r+1}$	$p_{r-2r,r+2}$	$p_{r-2r,r+3}$
$p_{r+1,r-1}$	$p_{r+1,r}$	$p_{r+1,r+1}$	$p_{r+1,r+2}$	$p_{r+1,r+3}$
$p_{r+2,r-1}$	$p_{r+2,r}$	$p_{r+2,r+1}$	$p_{r+2,r+2}$	$p_{r+2,r+3}$
$p_{r+3,r-1}$	$p_{r+3,r}$	$p_{r+3,r+1}$	$p_{r+3,r+2}$	$p_{r+3,r+3}$

Figure 4. The indices of pixels for a 3x3 window (r=1).

3. Classifiers

Fisher's Linear Discriminant Analysis is a well-known algorithm in pattern recognition field and it is used to find linear combination of features that categorizes classes of events. This algorithm is mostly used for two purposes that are linear classifier and dimensionality reduction. It projects data to find linear combinations with large ratios of between-class to within-class scatters. This ratio is referred as covariance matrix. According to Fisher's criteria, a covariance matrix is calculated by multiplying the inverse of the within-class covariance and between-class covariance. The inter-class difference is maximized by means of this new covariance matrix.

Linear Bayes Normal Classifier is another algorithm applied in this study. In this method, a linear classifier is computed between classes that have normal densities with equal covariance matrices. The joint covariance matrix is weighted using class covariance matrices. A regularization is applied to eliminate small variance directions and then a new covariance matrix is computed via the leading principal components and smallest eigenvalues [19].

Decision Tree has decision nodes, branches, and leaf nodes that are referred as features, conditions, and classes, respectively. Information gain or purity are used to create nodes. Conditions (branches) are utilized to determine the following node. Algorithm proceeds with the related branch considering the correctness of the condition, however if the condition is false, it jumps into the other branch. Finally, a leaf node is reached and then the class information is obtained.

K-Nearest Neighbor has a lazy learning and it is a distance based classifier. Classification procedure is carried out according to the similarities of events. An event is assigned to a class that is the most common amongst its k-neighbor classes.

Table 1. Time domain features

Feature Index	*Feature Name*	*Mathematical Representation*
f_1	Gray Level	$p_{r+1,r+1}$
f_2	Edge Magnitude	$\sqrt{dfx^2 + dfy^2}$ $dfx = (p_{r+2,r} + 2p_{r+2,r+1} + p_{r+2,r+2}) - (p_{r,r} + 2p_{r,r+1} + p_{r,r+2})$ $dfy = (p_{r,r+2} + 2p_{r+1,r+2} + p_{r+2,r+2}) - (p_{r,r} + 2p_{r+1,r} + p_{r+2,r})$
f_3	Edge Direction	$\tan^{-1}\left({}^{dyf}/_{dyx}\right)$
f_4	Maximum	$max\{p_{u,v} \mid u,v = 1,2,\dots,2r+1\}$
f_5	Minimum	$min\{p_{u,v} \mid u,v = 1,2,\dots,2r+1\}$
f_6	Average (μ)	${}^{1}/_{(2r+1)^2} \sum_{u=1}^{2r+1}\sum_{v=1}^{2r+1} p_{u,v}$
f_7	Variance	${}^{1}/_{(2r+1)^2} \sum_{u=1}^{2r+1}\sum_{v=1}^{2r+1} (p_{u,v} - \mu)^2$
f_8	Standart Deviation (σ)	$\sqrt{Variance}$
f_9	Area Descriptor	${}^{(\sigma)}/_{(\mu)}$
f_{10}	Moments	$\frac{1}{m_1}\left[\frac{1}{N}\sum_{i=1}^{N}(z_i - m_1)^4\right]^{1/4} - \left[\frac{1}{N}\sum_{i=1}^{N}(z_i - m_1)^2\right]^{1/2}$
f_{11}	Busyness	$\frac{1}{4r(2r+1)}\left[\sum_{u=1}^{2r+1}\sum_{v=1}^{2r+1}\lvert p_{u,v} - p_{u,v+1}\rvert + \sum_{u=1}^{2r+1}\sum_{v=1}^{2r+1}\lvert p_{u,v} - p_{u+1,v}\rvert\right]$
f_{12}	Entropy	$p(1-p)$, $p = \frac{p_{r+1,r+1}}{\sum_{u=1}^{2r+1}\sum_{v=1}^{2r+1}(p_{u,v})}$
f_{13}	Skewness	$\frac{1}{4r(r+1)\sigma^3}\sum_{u=1}^{2r+1}\sum_{v=1}^{2r+1}(p_{u,v} - \mu)^3$
f_{14}	Kurtosis	$\frac{1}{4r(r+1)\sigma^4}\sum_{u=1}^{2r+1}\sum_{v=1}^{2r+1}(p_{u,v} - \mu)^4$
f_{15}	Average Boundary Gray (μ_2)	*Average gray level value around the outside of the window*
f_{16}	Difference (ε)	$\mu - \mu_2$
f_{17}	Contrast	$\varepsilon/\mu + \mu_2$

4. Experimental Study

In this paper, the detection of the symptoms for DR disease from fundus images is proposed. First of all, 68 features are extracted from generated database that has 185 images with 5 classes. Secondly, classification is performed with all features. FLDA, LDC, DT and k-NN are used and the recognition accuracies are obtained. Thirdly, a feature selection method (SFS) is performed on all features and ultimately, the fundus images are again classified via same classifiers.

4.1. Database

A publicly available fundus image database that is DIARETDB1 is used [7]. This database includes 5 classes which are normal, mild, moderate, severe non-proliferative and proliferative DR. It has 89 fundus images (5 normal, 84 have non-proliferative and proliferative DR). These images have a size of 1500x1152. Each image is masked and preprocessed by some image processing operations and then they are saved in ".png" format. Besides, the ground-truths of them are provided. A new database is generated from ground-truths of those images. This new database has 185 images with 5 classes which are the same as abovementioned classes. The classes and the number of images are given in Table 2.

Table 2. Generated database

Class Name	*Total Number of Fundus Images*
Normal	23
Micro-Aneurysm	41
Hemorrhages	46
Hard Exudates	44
Soft Exudates	31

4.2. Feature Vector Construction

All fundus images in the database are separated into patches for the ease of extracting features. One image has divided into four patches and each of them has equal size of 375x288. The time-domain features, given in Table 1, are computed from each patch. The average (mean) values of features are calculated from four patches for each fundus image and they are treated as feature vector for corresponding fundus image.

4.3. Classification

The generated database is divided into a training and a test sets which have 80% and 20% of the number of images in the database, respectively. The five-fold cross-validation is conducted while classification is performed by four different classifiers using MATLAB PRtools toolbox [19]. Then, the Sequential Feature Selection algorithm is applied to the training dataset. During this stage, the "sequentialfs.m" function in MATLAB is carried out and the criteria for feature selection is accuracy results from classification. Classification with four different classifier is repeated with only selected features for comparison.

4.4. Performance Evaluation

The classification results for all folds without feature selection (68 features) are shown in Table 3. All calculated accuracy values are higher than 90%. k-NN gives the best results while using all features. The mean accuracy is 92.22% for k-NN, and DT is following it with a mean accuracy of 91.24%. For other classifiers, the mean accuracy values are 90.59% (FLDA) and 91.03% (LDC).

Table 6. The classification accuracies and the number of selected features

Classifier	***FLDA***		***LDC***		***k-NN***		***DT***	
Folds	#	Acc.	#	Acc.	#	Acc.	#	Acc.
Fold 1	15	95.14	6	92.97	1	87.57	4	90.81
Fold 2	13	92.43	7	96.22	1	85.41	4	92.97
Fold 3	6	91.35	5	95.14	1	88.11	4	94.05
Fold 4	11	90.27	4	88.11	1	87.03	5	91.89
Fold 5	12	91.35	6	90.27	1	85.95	6	89.19
Average Accuracy	92.12		92.54		86.81		91.78	

Table 3. The classification accuracies with all features

	Classification Accuracies (%)					
Classifier	***1.Fold***	***2.Fold***	***3.Fold***	***4.Fold***	***5.Fold***	***Average***
FLDA	89.73	90.27	91.89	90.81	90.27	90.59
LDC	92.43	91.35	91.89	89.19	90.27	91.03
DT	90.27	93.51	92.43	88.65	91.35	91.24
k-NN	94.05	94.60	92.43	88.65	91.35	92.22

After SFS is applied, the indices of the selected features are shown in Tables 4 and 5.

Table 4. The indices of selected features for FLDA

	FLDA
Fold 1	$f_2, f_4, f_7, f_8, f_{11}, f_{12}, f_{14}, f_{18}, f_{25}, f_{29}, f_{30}, f_{47}, f_{48}, f_{56}, f_{66}$
Fold 2	$f_1, f_2, f_7, f_8, f_{14}, f_{24}, f_{30}, f_{41}, f_{42}, f_{47}, f_{50}, f_{51}, f_{63}$
Fold 3	$f_3, f_{30}, f_{41}, f_{47}, f_{67}, f_{68}$
Fold 4	$f_3, f_{12}, f_{16}, f_{17}, f_{24}, f_{29}, f_{47}, f_{51}, f_{60}, f_{64}, f_{67}$
Fold 5	$f_3, f_{13}, f_{14}, f_{24}, f_{33}, f_{46}, f_{48}, f_{58}, f_{64}, f_{65}, f_{67}$

Table 5. The indices of selected features for DT, LDC, k-NN

	k-NN	***DT***	***LDC***
Fold 1	f_{14}	$f_{14}, f_{24}, f_{55}, f_{63}$	$f_7, f_{12}, f_{17}, f_{26}, f_{50}, f_{58}$
Fold 2	f_{47}	$f_{13}, f_{50}, f_{58}, f_{65}$	$f_{17}, f_{29}, f_{46}, f_{58}, f_{64}, f_{65}, f_{68}$
Fold 3	f_{22}	$f_{24}, f_{29}, f_{31}, f_{67}$	$f_{12}, f_{17}, f_{41}, f_{47}, f_{68}$
Fold 4	f_{58}	$f_{12}, f_{25}, f_{47}, f_{50}, f_{56}$	$f_{16}, f_{46}, f_{62}, f_{68}$
Fold 5	f_{21}	$f_3, f_7, f_{22}, f_{41}, f_{47}, f_{50}$	$f_3, f_{16}, f_{17}, f_{41}, f_{47}, f_{68}$

The accuracies for all folds after selection are shown in Table 6. FLDA has used maximum 15 features (only 22% of all features) and accuracies for all folds are increased. The mean accuracy after feature selection is 92.12% for FLDA. The mean accuracy is also amplified for LDC. It uses maximum 7 features, which is less than that of FLDA, and its mean accuracy increased by 1%. In addition to these results, mean accuracy for DT is almost the same, however it gives these approximately same results with maximum 6 features. On the contrary of these classifiers, mean accuracy of k-NN is decreased by 5% and it exposes the worst recognition. The classification results and total number of selected features for each classifier and fold are explicitly shown in Table 6.

5. Conclusion

In this study, four different classifiers are compared in terms of accuracy and number of selected features on the DIARETDB1 database. The aim is to find the most appropriate classifier and feature set for detecting symptoms of DR. As a conclusion, it is deduced that k-NN is superior to all other methods for detecting MA, HR, SE, HE symptoms by using 68 features. Besides, DT provides nearly same performance with all features. After the usage of selected features, DT gives nearly same results, but the accuracies of FLDA and LDC are prominently increased with considerably less features.

References

[1] Jagadish Nayak et al. (2007). Automated Identification of Diabetic Retinopathy Stages Using Digital Fundus Images. Journal of Medical System. Vol. 32. Pages. 107-115.

[2] Ronald Klein, Barbara E.K. Klein, Susan C. Jensen and Scot E. Moss (2001). The relation of socioeconomic factors to the incidence of early age-related maculopathy: The Beaver Dam Eye Study. American Journal of Ophthalmology. Vol. 132. Pages. 128–131.

[3] Ankita Agrawal, Charul Bhatnagar and Anand Singh Jalal (2013). A Survey on Automated Microaneurysm Detection in Diabetic Retinopathy Retinal Images. Information Systems and Computer Networks (ISCON). Pages. 24-29.

[4] Micheal D. Abramoff, Mona K. Garvin and Milan Sonka (2010). Retinal Imaging and Image Analysis. IEEE Reviews in Biomedical Engineering. Vol. 3. Pages. 169-208.

[5] Akara Sopharak, Bunyarit Uyyanonvara, Sarah Barman and Thomas H. Williamson (2008). Automatic Detection of Diabetic Retinopathy Exudates from Non-Dilated Retinal Images Using Mathematical Morphology Methods. Computerized Medical Imaging and Graphics. Vol. 32. Pages. 720–727.

[6] Diptoneel Kayal and Sreeparna Banerjee (2014). A New Dynamic Tresholding Based Technique for Detection of Hard Exudates in Digital Retinal Fundus Image.

International Conference on Signal Processing and Integrated Networks (SPIN). Pages.141-144.

[7] T.Kauppi et al. DIARETDB1 diabetic retinopathy database and evaluationprotocol. Available: http://www.it.lut.fi/project/ imageret/diaretdb1/.

[8] M. Usman Akram, Shehzad Khalid and Shoab A. Khan (2013). Identification and classification of microaneurysms for early detection of diabetic retinopathy. Pattern Recognition. Vol. 46. Pages. 107-116.

[9] Kanika Verma, Prakash Deep and A.G. Ramakrishnan (2011). Detection and Classification of Diabetic Retinopathy using Retinal Images. India Conference (INDICON). Pages. 1-6.

[10] Marwan D. Saleh and C. Eswaran (2012). An Automated Decision-Support System for Non-Proliferative Diabetic Retinopathy Disease Based on MAs and Has detection. Computer Methods and Programs in Biomedicine. Vol. 108. Pages. 186-196.

[11] Wong Li Yun et. al. (2008). Identification of Different Stages of Diabetic Retinopathy Using Retinal Optical Images. Information Sciences. Vol. 178. Pages. 106-121.

[12] Maria Garcia, Roberto Hornero, Clara I. Sánchez, María I. López and Ana Díez (2007). Feature Extraction and Selection for the Automatic Detection of Hard Exudates in Retinal Images. Proceedings of the 29th Annual International Conference of the IEEE EMB. Pages. 4969-4972.

[13] Mahendran Gandhi and Dr. R. Dhanasekaran (2013). Diagnosis of Diabetic Retinopathy Using Morphological Process and SVM Classifier. International conference on Communication and Signal Processing, India. Pages. 873-877.

[14] R. A. Fisher Sc.D., F.R.S. (1936). The Use of Multiple Measurements in Taxonomic Problems. Annuals of Eugenics. Vol. 7. Pages. 179-188.

[15] Richard O. Duda, Peter E. Hart, and David G. Stork (2001). Pattern Classification 2nd edition. John Wiley and Sons, New York.

[16] J.R. Quinlan (1987). Simplifying Decision Trees. International Journal of Man-Machine Studies. Vol. 27. Pages. 221-234.

[17] T. Cover and P. Hart (1967). Nearest Neighbor Pattern Classification. IEEE Transactions on Information Theory. Vol. 13. Pages. 21-27.

[18] Nikhil R. Pal, Brojeshwar Bhowmick, Sanjaya K. Patel, Srimanta Pal and J. Das (2008). A Multi-Stage Neural Network Aided System for Detection of Microcalcifications in Digitized Mammograms. Neurocomputing. Vol. 71. Pages. 2625-2634.

[19] R.P.W. Duin et. al. PRTools4 A Matlab Toolbox for Pattern Recognition.Available: http://prtools.org.

